Resonant inhomogeneous molecular absorption of ultrashort laser pulses: role of the pulse spectrum

Pritish Mukherjee

Laboratory for Applied Laser Research, Department of Physics, University of South Florida, Tampa, Florida 33620

Hoi S. Kwok

Department of Electrical & Computer Engineering, State University of New York at Buffalo, Amherst, New York 14260

Received March 20, 1992; revised manuscript received September 28, 1992

A model molecular system composed of an inhomogeneous distribution of homogeneous wave packets is presented in analogy with gain saturation in atomic systems. The numerically computed optical free-induction-decay pulse spectrum (as a representative picosecond-pulsed laser system) and other idealized pulse spectra are used as inputs to the molecular system to probe its absorption characteristics in the inhomogeneous limit. Various aspects of pulse spectral structure and their relative significance to the observed nonlinearity of the numerically computed $1/\sigma^2$-versus-I plot is discussed in detail. The relevance of such behavior in interpreting experimental data is also indicated.

INTRODUCTION

The absorption of laser radiation by molecular systems yields, on careful investigation, fundamentally valuable information about various mechanisms responsible for energy transfer into molecules. Specifically, the use of infrared lasers to excite various vibrational modes of a polyatomic molecule is well known (see, for example, Refs. 1–5). Of particular interest is a study of the collisionless interaction of laser light with the molecule. Such studies are possible by suitable adjustment of the pressure of the experimental gas and/or by use of ultrashort picosecond laser pulses. The use of short pulses permits a total absence of collisions during the picosecond laser pulse, as the gas kinetic collision time (typically 25 ns Torr) is much longer than the pulse duration. It has been shown[6] that a study of the saturation characteristics of the absorption of laser energy by the molecule, in a collisionless manner, permits the modeling of the absorption in terms of a multitier set of states. It was found that the laser was strongly coupled to the molecule via the first-tier states. For C_2F_5Cl an inhomogeneously broadened absorption implied essential decoupling of the first-tier states. In any such modeling it is quite obvious that the saturation characteristics (i.e., whether the broadening is homogeneous or inhomogeneous) dictate the extent of coupling between the first-tier states.

In this study we analyze the effect of spectral structure of the pulse on the absorption characteristics of the molecular system. The primary motivation for such a study is to determine the extent of influence in the frequency domain exercised by the actual pulse shape in terms of modifying the experimentally observed saturation of the absorption cross section. Specifically, we focus on the saturation characteristics as exhibited by the variation of $1/\sigma^2$ with the peak laser intensity in the frequency domain. It is shown that an accurate interpretation of saturation data should incorporate the spectral distribution of intensity of the experimental laser pulse. A well-known theoretical model for atomic systems,[7] involving an inhomogeneous ensemble of homogeneous wave packets, is analogously used to model the molecular system. Numerical calculations for the absorption cross sections of various mathematically tailored spectral pulse shapes and an actual pulse profile [the picosecond optical free-induction-decay (OFID) pulse] are presented. A comparative analysis of the various calculations reveals that there is an intensity-dependent modification of the overall saturation characteristics for the OFID pulse because of its spectral extent.

MODEL

In order to study the effects of various spectral structures on the absorption it is necessary to model the molecular system appropriately. The importance of small-signal experiments to probe dissociationless, vibrational excitation in polyatomic molecules has been demonstrated.[6,8,9] Under small-signal conditions it is possible to model the molecule as a two-level system. The motivation for such a scheme is that if the absorption is, on an average, subphoton per molecule, then at most two levels related by a single-photon transition are involved in the absorption process. More precisely, the small-signal limit may be designated as the intensity regime in which the two-level rate-equation approach is valid. In this case the Rabi frequency ($\omega_R = \mu E/\hbar$, where μ is the dipole moment and E the electric field of the laser) is less than the molecular transition linewidth; i.e., $\omega_R < \Delta\omega$. In the present model we consider an inhomogeneous system that comprises homogeneous wave packets. The concept is adequately elucidated in Ref. 7. The considerations that apply to atomic transitions there are extended here to the molecular absorption line shape. We consider the inhomoge-

0740-3224/93/030425-08$05.00

neous line shape to be made up of classes of intramolecular transitions, each designated by a center frequency ν_ξ. The function $p(\nu_\xi)$ is defined so that the probability that the transition has its center frequency between ν_ξ and $\nu_\xi + d\nu_\xi$ is given by $p(\nu_\xi)d\nu_\xi$. Assuming that each transition in the class ξ is identical, a homogeneous Lorentzian line-shape function $l(\nu)$ with a width $\Delta\nu$ may be used to represent each individual inhomogeneous line. Such an ensemble of inhomogeneously distributed homogeneous wave packets may be denoted by an absorption cross section,

$$\sigma(\nu) = \frac{c^2\Delta N_0\Delta\nu}{16\pi^2n^2\nu^2t_{\text{spont}}}\int_{-\infty}^{\infty}\frac{p(\nu_\xi)d\nu_\xi}{(\nu-\nu_\xi)^2+\left(\frac{\Delta\nu}{2}\right)^2+\frac{\phi c^2I_\nu\Delta\nu}{8\pi^2n^2h\nu^3}}, \tag{1}$$

analogous to Ref. 7. In the above expression, ΔN_0 is the number density of absorbers, c is the velocity of light, I_ν is the laser intensity at a frequency ν, h is Planck's constant, n is the refractive index of the molecular medium, t_{spont} is the lifetime that is due to spontaneous transitions, and $\phi = \tau/t_{\text{spont}}$, where τ is the inversion lifetime.

The overall absorption cross section of the laser pulse (including its various frequency components) by the molecule is given by

$$\sigma = \frac{\int I_\nu\sigma(\nu)d\nu}{\int I_\nu d\nu}. \tag{2}$$

The knowledge of the laser intensity in the frequency domain combined with Eq. (1) therefore permits the determination of the resultant absorption cross section of the laser pulse for varying peak laser intensities.

Since we are interested only in the frequency-dependent component of $\sigma(\nu)$, all the terms that are independent of ν are lumped together as a constant K so that Eq. (1) may be simplified to

$$\sigma(\nu) = \frac{K\Delta\nu}{\nu^2}\int_{-\infty}^{\infty}\frac{p(\nu_\xi)d\nu_\xi}{(\nu-\nu_\xi)^2+\left(\frac{\Delta\nu}{2}\right)^2+\frac{\phi c^2I_\nu\Delta\nu}{8\pi^2n^2h\nu^3}}. \tag{3}$$

A Gaussian line shape with a width $\Delta\nu_i$ is used to represent the inhomogeneous distribution $p(\nu_\xi)$, leading to

$$\sigma(\nu) = \frac{K\Delta\nu}{\nu^2}\int_{-\infty}^{\infty}\frac{\exp(-2.77(\nu_0-\nu_\xi)^2/(\Delta\nu_i)^2)d\nu_\xi}{(\nu-\nu_\xi)^2+\left(\frac{\Delta\nu}{2}\right)^2+\frac{\phi c^2I_\nu\Delta\nu}{8\pi^2n^2h\nu^3}}, \tag{4}$$

where ν_0 is the central laser frequency. This approach centers the inhomogeneous absorption line shape at the central laser frequency. Experimentally, this implies resonance of the central laser frequency with the molecular absorption. A representation of the model molecular system is shown in Fig. 1. In general, therefore, the frequency of the laser radiation may be denoted by

$$\nu = \nu_0 + \nu', \qquad \nu > \nu_0,$$
$$\nu = \nu_0 - \nu', \qquad \nu < \nu_0, \tag{5}$$

and I_ν denotes the laser intensity at a frequency shifted from the central frequency ν_0 by ν'.

Equation (4) may be written in a suitable manner for contributions from the two halves of the laser-pulse spectrum by using the transformation $\nu_\xi - \nu_0 - \nu' = \alpha$. After some elementary algebra, Eq. (4) leads to

$$\sigma_+(\nu) = \frac{K\Delta\nu}{(\nu_0+\nu')^2}\left[\int_0^{\infty}\frac{\exp(-2.77(\nu'-\alpha)^2/(\Delta\nu_i)^2)d\alpha}{\alpha^2+\left(\frac{\Delta\nu}{2}\right)^2+\frac{\phi c^2I_\nu\Delta\nu}{8\pi^2n^2h(\nu_0+\nu')^3}} + \int_0^{\infty}\frac{\exp(-2.77(\nu'+\alpha)^2/(\Delta\nu_i)^2)d\alpha}{\alpha^2+\left(\frac{\Delta\nu}{2}\right)^2+\frac{\phi c^2I_\nu\Delta\nu}{8\pi^2n^2h(\nu_0+\nu')^3}}\right] \tag{6a}$$

for the right half of the spectrum (i.e., $\nu > \nu_0$) and

$$\sigma_-(\nu) = \frac{K\Delta\nu}{(\nu_0+\nu')^2}\left[\int_0^{\infty}\frac{\exp(-2.77(\nu'+\alpha)^2/(\Delta\nu_i)^2)d\alpha}{\alpha^2+\left(\frac{\Delta\nu}{2}\right)^2+\frac{\phi c^2I_\nu\Delta\nu}{8\pi^2n^2h(\nu_0-\nu')^3}} + \int_0^{\infty}\frac{\exp(-2.77(\nu'-\alpha)^2/(\Delta\nu_i)^2)d\alpha}{\alpha^2+\left(\frac{\Delta\nu}{2}\right)^2+\frac{\phi c^2I_\nu\Delta\nu}{8\pi^2n^2h(\nu_0-\nu')^3}}\right] \tag{6b}$$

for the left half of the spectrum (i.e., $\nu < \nu_0$). For the whole pulse,

$$\sigma(\nu) = \sigma_+(\nu) + \sigma_-(\nu). \tag{6c}$$

The molecular absorbing system is now specified. However, a description of I_ν requires a realistic laser-pulse spectral profile, thereby completing the specification of the laser–molecule interaction. Since several small-signal absorption measurements[6,8,9] on polyatomic molecules have used the picosecond OFID laser output,[10,11] it is used as a realistic example here. The calculation of I_ν for the ultrashort pulse OFID laser output is detailed in Appendix A. Equations (6) are, however, quite general and amenable to any choice for I_ν, including purely idealistic mathematical pulse spectra.

Equation (A10) (in Appendix A), in conjunction with Eqs. (2) and (6), specifies the absorption problem completely.

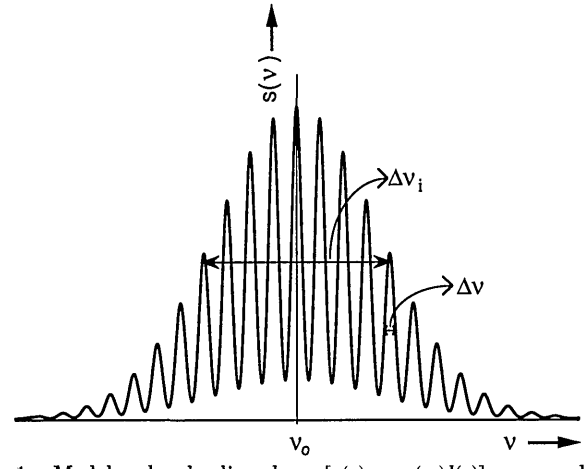

Fig. 1. Model molecular line shape $[s(\nu) = p(\nu_\xi)l(\nu)]$ composed of an inhomogeneously distributed ensemble of homogeneous wave packets (of FWHM $\Delta\nu$). The overall envelope, representing the inhomogeneous Gaussian distribution (of FWHM $\Delta\nu_i$), is in resonance with the central laser frequency at ν_0.

NUMERICAL RESULTS

Now that we have established the model molecular system and the realistic OFID laser pulse spectrum, it is reasonably straightforward to calculate the absorption cross section (σ) of the molecule as a function of peak intensity of the OFID temporal pulse profile, using Eqs. (5), (6), and (A10). Though the model developed above is generally true, we use it (for the purpose of the present calculations) to simulate an inhomogeneously broadened case. For this to be true the condition

$$\Delta\nu_i \gg \Delta\nu \tag{7}$$

must be satisfied. This would imply that the width of the inhomogeneous Gaussian profile, being large, causes the function $p(\nu_\xi)$ to remain essentially constant over the region in which the integrand in Eq. (1) peaks. For such a case, as in Ref. 7, one may write the absorption cross section as

$$\sigma(\nu) = \frac{Kp(\nu)}{\nu^2}\int_{-\infty}^{\infty} \frac{d\nu_\xi}{(\nu-\nu_\xi)^2 + \left(\frac{\Delta\nu}{2}\right)^2 + \frac{\phi c^2 I_\nu \Delta\nu}{8\pi^2 n^2 h\nu^3}}, \tag{8}$$

using Eq. (4). Thus, analytically, $\sigma(\nu)$ is expressible in the form[7]

$$\sigma(\nu) = [\sigma_0(\nu)]/\{1 + I_\nu/[I_{sat}(\nu)]\}^{1/2}, \tag{9}$$

where

$$\sigma_0(\nu) = [\pi K p(\nu)]/\nu^2, \tag{10a}$$

$$I_{sat}(\nu) = (2\pi^2 n^2 h\nu^3 \Delta\nu)/\phi c^2. \tag{10b}$$

$\sigma_0(\nu)$ and $I_{sat}(\nu)$ are the small-signal absorption cross section and the saturation intensity at a frequency ν, respectively.

In the numerical simulation of the inhomogeneously broadened system the general equations (5), (6), and (A10) are used with values of $\Delta\nu$ and $\Delta\nu_i$ fixed at 0.25 and 400 GHz, respectively, in order to satisfy the validity of Eq. (7) and consequently Eq. (9). This ensures that each frequency component of the laser pulse sees an inhomogeneously broadened absorption. Additionally, these values are consistent with typical molecular parameters for polyatomic molecules in their vibrational quasicontinua.[3,4,8,9] The value of ϕ is used to adjust I_{sat} [as defined by Eqs. (10)] to ensure that the effects of saturation are manifest for the range of I_ν used. ϕ was set equal to 10^{-7} throughout the present numerical simulations. A change in the value of ϕ would merely result in the saturation effects' being evident at an altered peak temporal intensity. The ultimate conclusions of this study are, however, independent of the specific value of ϕ chosen.

From Eq. (9) it follows that, if the overall absorption of the laser radiation by the molecule is indeed inhomogeneous, then

$$\frac{1}{\sigma^2} = \frac{1}{{\sigma_0}^2} + \frac{I}{{\sigma_0}^2 I_{sat}}, \tag{11}$$

thereby leading to a linear plot of $1/\sigma^2$ versus I. Figure 2 shows the results of a numerical calculation made with the OFID spectrum illustrated in Fig. 12 below. The interesting observation is that the plot of $1/\sigma^2$ versus I shows a distinct departure from linearity as the intensity is augmented. Figure 3 shows the linearity of $1/\sigma(\nu)^2$ versus I_ν for three different spectral components of the OFID spectrum. These three plots correspond to (a) the central frequency ν_0, (b) the frequency (ν_{max}) at which I_ν is a maximum, and (c) a frequency (ν_t) in the tail of the OFID spectrum. At each of these individual frequencies, separated from one another in frequency and distinct in intensity, the absorption is purely inhomogeneous, as expected. The overall absorption does not, however, follow the $1/\sigma^2$ versus I linearity characteristically expected of the inhomogeneous case.

Two mechanisms were considered as possible explanations of such a behavior. Various tailored pulses were used as an input to the molecular system to probe these mechanisms. The first possibility considered was the effect of a variable intensity profile (as a function of frequency in the pulse spectrum) in causing the observed nonlinearity. The two cases considered were those of a rectangular pulse and of a triangular pulse in the frequency domain. Figures 4 and 5 show the resultant $1/\sigma^2$-versus-I plots. Though Fig. 5 does show some evidence of nonlinearity compared with the absolutely linear character of Fig. 4 (representing the rectangular pulse input), the effect is much less than that observed for the OFID pulse.

The second possibility explored was the effect of the tail in the pulse frequency spectrum. In order to study this effect comparatively, we selected three different pulse shapes. In each of these pulse shapes the linear rise was identical and its extent was tailored to simulate approximately the rise (in the frequency domain) of the

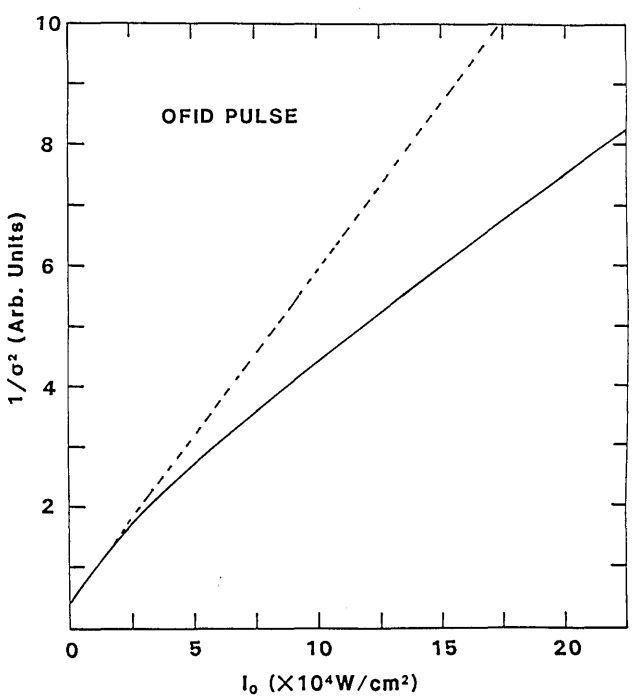

Fig. 2. $1/\sigma^2$ as a function of peak OFID laser intensity for an OFID pulse of duration 44 ps, depicted by the solid curve. An extrapolation of the trend exhibited by the lower-intensity values is shown by the dashed line.

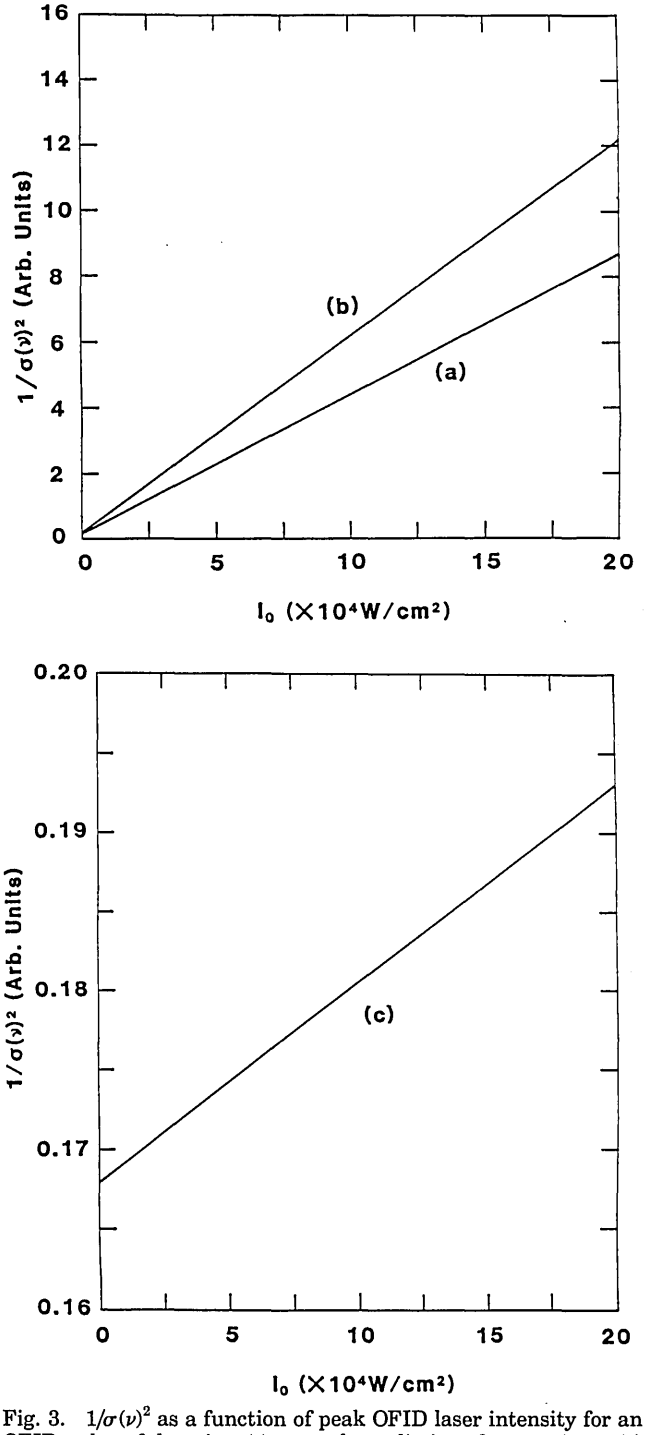

Fig. 3. $1/\sigma(\nu)^2$ as a function of peak OFID laser intensity for an OFID pulse of duration 44 ps at three distinct frequencies: (a) the central laser frequency (ν_0); (b) the frequency (ν_{max}) at which I_ν is a maximum, and (c) a frequency (ν_t) in the tail of the OFID pulse spectrum. Note the linearity of all the plots.

OFID pulse spectrum. The difference among the three cases was in the rate of fall of intensity; it corresponded to a linear, a semi-Gaussian, and a semi-Lorentzian fall, respectively. The resultant $1/\sigma^2$-versus-I plots shown in Figs. 6–8 show a progressively increasing nonlinear trend from linear to semi-Gaussian to semi-Lorentzian. The implication of the connection between a larger spectral tail and the observed nonlinearity is obvious.

In all the pulse shapes used the peak intensity (in the frequency domain) was kept constant. The width of the pulses was then adjusted so that, in each case,

$$\int_0^\infty I_\nu d\nu$$

had a constant value at the same I_0. This ensured that the overlapped area, in the frequency domain, was the

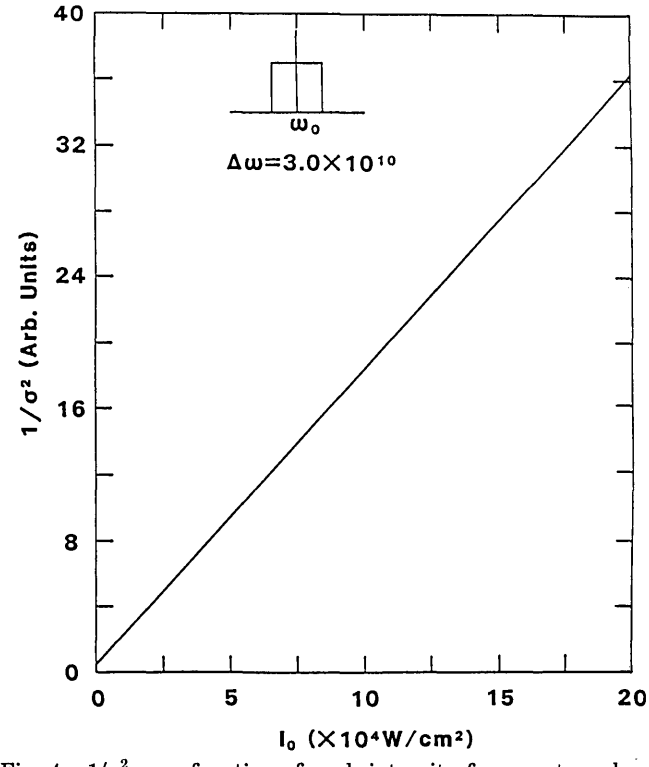

Fig. 4. $1/\sigma^2$ as a function of peak intensity for a rectangular pulse (in the frequency domain). Note the linearity of the plot.

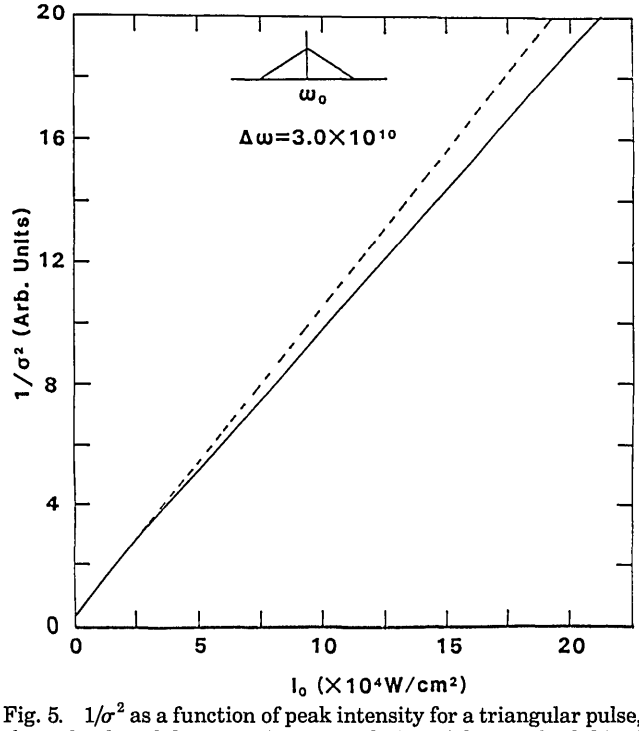

Fig. 5. $1/\sigma^2$ as a function of peak intensity for a triangular pulse, shown by the solid curve. An extrapolation of the trend exhibited by the lower intensity values is shown by the dashed line.

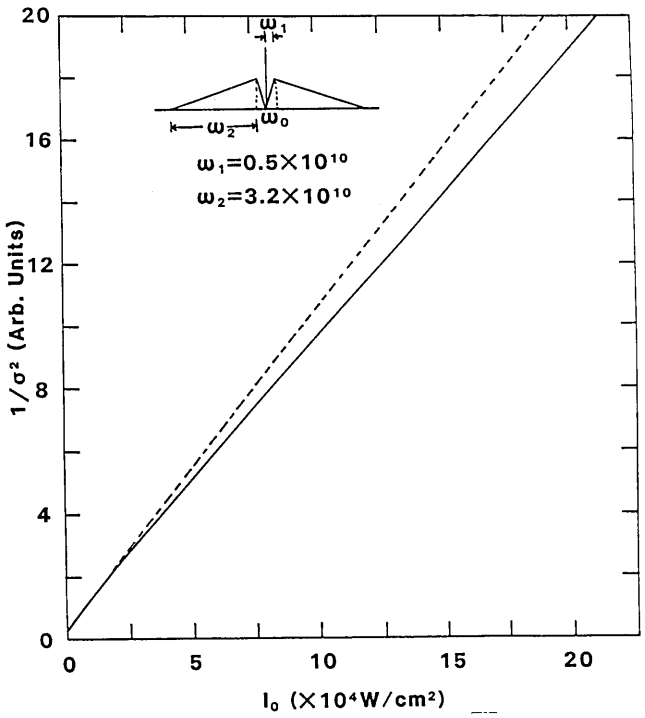

Fig. 6. $1/\sigma^2$ as a function of peak intensity for a triangular pulse, shown by the solid curve. An extrapolation of the trend exhibited by the lower-intensity values is shown by the dashed line. Note the departure from a linear plot. The input pulse shape with the relevant parameters is indicated in the inset.

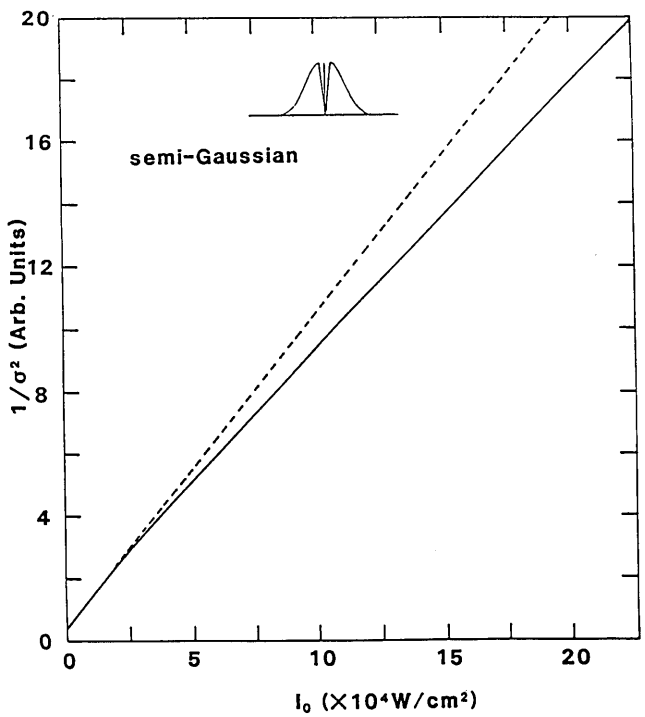

Fig. 7. $1/\sigma^2$ as a function of peak intensity for a semi-Gaussian pulse, shown by the solid curve. An extrapolation of the trend exhibited by the lower-intensity values is shown by the dashed line. Note the increasing departure from linearity compared to Fig. 6. The input pulse shape with the relevant parameters is indicated in the inset.

same for all the pulses studied. The individual pulse parameters are shown, with the appropriate pulse shape, as an inset in each of the relevant figures.

DISCUSSION

The two cases considered, that of varying laser intensity as a function of frequency in the pulse spectrum and that of a variable extent of the tail in the pulse spectrum, enable us to focus on the relative contributions of the two factors to the observed nonlinear behavior of the $1/\sigma^2$-versus-I plot. Even though the triangular pulse (whose pulse spectrum varies in intensity as a function of frequency) does result in some evidence of nonlinearity in Fig. 5, the departure from the constant intensity rectangular profile's linear plot is admittedly slight. On the other hand, Figs. 6–8 clearly demonstrate that the presence of a larger spectral tail is indeed instrumental in a significant departure from a linear plot. The clipped pulse profile of Fig. 6 demonstrates only a meager change in the linear $1/\sigma^2$-versus-I plot. The semi-Lorentzian fall shown in Fig. 8, on the other hand, possessing a larger wing than its clipped or semi-Gaussian counterpart (Fig. 7), shows a corresponding enhanced nonlinearity quite similar to that evidenced by the OFID pulse. On observation of the OFID pulse spectrum (Fig. 12), it is evident that the wings are more pronounced than that of a semi-Gaussian and slightly more than the semi-Lorentzian. The observed progression in nonlinearity bears out this fact.

One may understand the basic observations made here mathematically by using simple arguments. From Eqs. (10) we see that the slope $[m(\nu)]$ of the $1/\sigma(\nu)^2$-versus-I_ν plot is given by

$$m(\nu) = 1/[\sigma_0^2(\nu) I_{\text{sat}}(\nu)]\,. \tag{12}$$

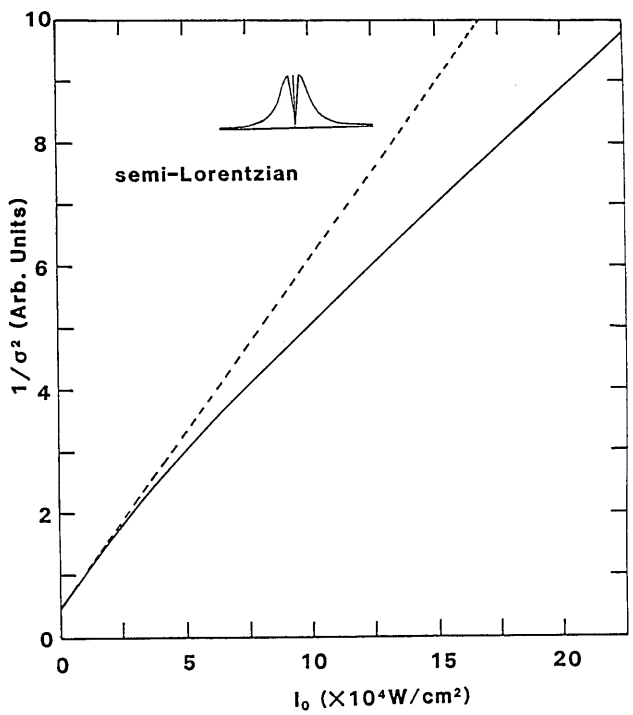

Fig. 8. $1/\sigma^2$ as a function of peak intensity for a semi-Lorentzian pulse, shown by the solid curve. An extrapolation of the trend exhibited by the lower-intensity values is shown by the dashed line. Note the large departure from linearity, greater than in Fig. 6 or 7 and approaching that of Fig. 2. Even though arbitrary units are used for $1/\sigma^2$, the values noted are relatively comparable in Figs. 2, 6, 7, and 8. The input pulse shape with the relevant parameters is indicated in the inset.

Using Eqs. (10a) and (10b) in the above expression, we may write

$$m(\nu) \alpha \nu/[p^2(\nu)]. \tag{13}$$

The value of ν specified for the laser pulse by Eqs. (5) enables us to represent the slope by

$$m(\nu) \alpha (\nu_0 + \nu')\exp[-2 \times 2.77(\nu')^2/(\Delta\nu_i)^2], \quad \nu > \nu_0,$$
$$m(\nu) \alpha (\nu_0 - \nu')\exp[-2 \times 2.77(\nu')^2/(\Delta\nu_i)^2], \quad \nu < \nu_0, \tag{14}$$

using the Gaussian representation for $p(\nu_\xi)$ given in Eq. (4). In general, since $\nu_0 \gg \nu'$, we may write an approximate unified expression for both the left and the right halves of the pulse spectrum as

$$m(\nu) \alpha \nu_o \exp[-2 \times 2.77(\nu')^2/(\Delta\nu_i)^2]. \tag{15}$$

Even though the asymmetry implied by relations (14) does exist, its effect is miniscule and does not alter the conclusions derived from relation (15).

Mathematically, relation (15) represents the fact that as ν' increases (thereby physically implying a progression toward the wings of the pulse spectrum), the slope of the individual $1/\sigma(\nu)^2$-versus-I_ν plot decreases. Each of these individual frequencies will, however, obey a linear $1/\sigma(\nu)^2$-versus-I_ν dependence. It is reasonable to expect that the combined effect of the individual frequencies would manifest itself in the overall $1/\sigma^2$-versus-I plot as a combinatorial effect (not necessarily additive) of the individual slopes. Therefore, as the intensity increases, the effect of the wings of the pulse spectrum will become more pronounced. As evidenced by relation (15), increased contribution from the wings will tend to *diminish* the slope. The observed decrease in slope of the $1/\sigma^2$-versus-I plots (in Figs. 2, 7, and 8) leading to a nonlinearity and its observed dependence on spectral structure are adequately described by the above considerations.

A comparison between the significance of the frequency tail of the pulse spectrum and the spectral extent of the pulse (measured by the FWHM) may readily be made by using Fig. 9. This figure superimposes the three distinct spectral pulse shapes used to generate the plots in Figs. 6–8. It is clearly evident that in the frequency domain the FWHM is largest for the pulse shape having the shortest tail, given a uniform peak spectral intensity and similar spectral overlap, as is the case here. Therefore the observed departure from linearity for longer tails may also, synonymously, be attributed to shorter FWHM of the frequency spectra. However, given the same peak intensity and FWHM, it is the tail of the spectral distribution that determines the extent of the observed nonlinear effect. This is obvious when one compares Figs. 4 and 5, where the triangular pulse (Fig. 5, with a longer tail) exhibits an effect not apparent for the rectangular pulse (Fig. 4). Both pulses, however, have the same FWHM, peak intensity, and spectral overlap. Therefore we can conclude that, though the FWHM of the spectral profile follows a progression that may be related to the observed effect just as readily as the frequency tail, it is the extent of the tail that is the primary determining factor.

An illustration of the basic idea that the wings of the pulse spectrum lead to the nonlinearity of the $1/\sigma^2$-versus-I plot is shown in Fig. 10. As we saw earlier in Fig. 4, in the frequency domain there was no deviation from linearity observed for a rectangular pulse. However, the addition of a low-intensity long tail (still maintaining the same spectral overlap) does cause a significant departure from a linear behavior. An interesting observation about Fig. 10 is the increased abruptness of departure from linearity compared with the OFID, semi-Lorentzian, or semi-Gaussian curves shown in Figs. 2, 7, and 8. The observed abruptness is due to the fact that the spectral profile of the rectangular pulse with a tail has an abrupt change in intensity. On the $1/\sigma^2$-versus-I plot the intensity at which the noticeable change occurs corresponds therefore to the intensity at which the contribution that is due to the tail achieves a significant weight. A smoothly graded intensity profile would evidently exhibit a less abrupt change from linearity, as successive initially insignificant contributions from the frequency wings become important with increasing peak intensity in a smoother fashion.

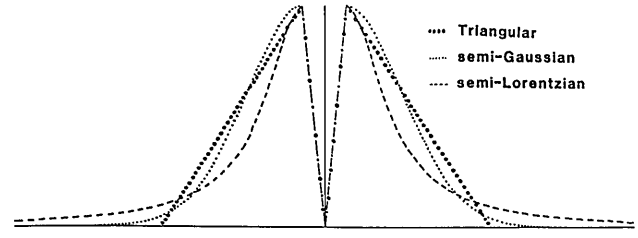

Fig. 9. Superimposed representation of the three pulse shapes used to generate Figs. 6–8, demonstrating the variable tail characteristic of the pulse spectra.

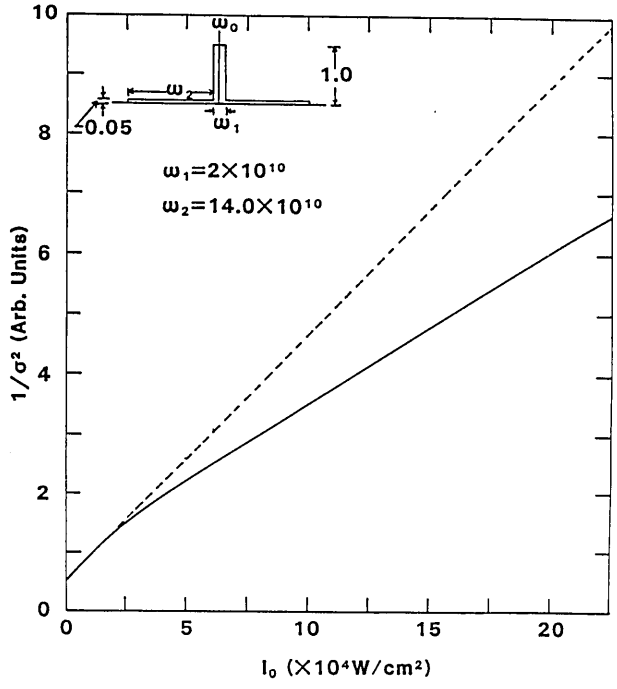

Fig. 10. $1/\sigma^2$ as a function of peak intensity for a rectangular pulse with a large frequency tail, shown by the solid curve. The pulse shape and relevant pulse parameters are shown in the inset. Note the large deviation from the low-intensity trend, extrapolated by the dashed line, indicative of the significant effect of a tail in the pulse spectrum.

CONCLUSION

In this paper we have presented a model that can represent adequately the absorption of laser radiation (with a finite spectral spread) by a molecular system. This model is analogous to that used in Ref. 7 to describe the saturation of gain of atomic systems. In its inhomogeneous limit the model was used to study the effect of variable intensity spectral profiles on the characteristics of the absorption. The use of various tailored pulse shapes in conjunction with a realistic OFID picosecond pulse spectrum as an input to the model molecular system clearly demonstrates the importance of the wings of the spectral shape in leading to a nonlinear behavior of the $1/\sigma^2$-versus-I plot for the absorption, contrary to the linearity expected of an inhomogeneous system. This nonlinearity was shown to be due to the cumulative effect of a frequency-dependent distribution of saturation intensities and small-signal absorption cross sections, a factor that is enhanced for variable intensity pulses with larger spectral extent.

The implication of the observed dependence of the spectral parameters of the pulse on an interpretation of absorption measurements vis-à-vis their inhomogeneous characteristic does have some experimental consequence. It is obvious that, in an interpretation of experimental absorption data, even when a two-level model is operative there is a necessity for caution in diagnosing the nature of the absorption. Even though the molecular system may respond in an inhomogeneous manner to each frequency component separately, the combined pulse absorption over all frequencies in the pulse spectrum may exhibit apparently noninhomogeneous characteristics. Therefore for an accurate interpretation it is relevant to consider the spectral structure of the particular pulse used for the experiments.

Even though the discussion presented in this paper has been based on a specific picosecond laser pulse spectrum (the OFID CO_2 laser pulse), the general conclusions regarding the effect of pulse spectral spread on the observed saturation characteristics are applicable to any ultrashort-pulse laser system. The nonlinear effects exhibited in our calculations will be more pronounced in experimental measurements, as the laser pulse spectrum broadens to overlap several inhomogeneous molecular absorption line shapes, a condition readily satisfied in the absorption of subpicosecond laser radiation by a polyatomic molecule, specifically under high levels of vibrational excitation into the quasi-continuum. The magnitude of the departure from linearity and a detection of its effect in a realistic situation will ultimately rest, of course, on the intensity range investigated and on the sensitivity of the experimental arrangement used.

In this paper we have presented a calculation of the absorption characteristics based on a knowledge of the molecular line shape and the laser-pulse spectrum. An interesting possibility would be an attempt to deduce the spectral profile of ultrashort laser pulses by coupling knowledge of the molecular absorption line shape with an experimental measurement of the abosrption characteristics. It is speculated that the experimental measurement of such a nonlinearity in two-level absorption characteristics may permit the indirect deduction of information about the spectral profiles of ultrashort pulses. The uniqueness of the outcome of such a deconvolution procedure remains to be established.

APPENDIX A

The frequency spectrum of the OFID pulse may be evaluated readily. When a truncated pulse (shown in Fig. 11) denoted by

$$E(t) = E_0 \exp[-(2 \ln 2)t^2/t_p^2], \quad t < 0,$$
$$E(t) = E_0 \exp[-(2 \ln 2)t^2/t_s^2], \quad t > 0 \tag{A1}$$

is used, where t_p is the FWHM of the intensity temporal profile and t_s the plasma shutter speed, evaluation of the Fourier transform leads to

$$F(\nu) = (\pi/8 \ln 2)^{1/2} E_0 \{t_p \exp(-4\pi^2\alpha^2 t_p^2 \nu^2) \times [1 - \phi(i\alpha 2\pi\nu t_p)] + t_s \exp(-4\pi^2\alpha^2 t_s^2 \nu^2) \times [1 - \phi(-i\alpha 2\pi\nu t_s)]\}, \tag{A2}$$

where $\alpha = 0.425$ and $\phi(z)$ is the complex error function denoted by

$$\phi(z) = \frac{2}{\sqrt{\pi}} e^{-z} \sum_{k=0}^{\infty} \frac{2^k z^{2k-1}}{(2k+1)!!}. \tag{A3}$$

Such a truncated pulse is characteristic of the output from the plasma shutter in an OFID system.[12] The transfer function of the hot cell, through which the truncated pulse subsequently passes, is given by[10]

$$H(\nu) = \exp\left[\frac{N}{2(1 + 2\pi i\nu T_2)}\right], \tag{A4}$$

where N is the hot cell absorption in nepers and T_2 is the dephasing time of the hot CO_2 molecules given by

$$\frac{1}{\pi T_2} = 7.58(300/T)^{1/2} \quad \text{MHz/Torr}, \tag{A5}$$

where T is the temperature of the CO_2 molecules. The resultant spectrum of the OFID pulse is therefore given by

$$S(\nu) = F(\nu)H(\nu), \tag{A6}$$

leading to an OFID pulse intensity spectrum

$$I(\nu) = |F(\nu)H(\nu)|^2 = \frac{\pi I_0}{8 \ln 2} |\{t_p \exp(-4\pi^2\alpha^2 t_p^2 \nu^2)[1 - \phi(i\alpha 2\pi\nu t_p)] + t_s \exp(-4\pi^2\alpha^2 t_s^2 \nu^2)[1 - \phi(-i\alpha 2\pi\nu t_s)]\}|^2 \times \exp\left(\frac{N}{1 + 4\pi^2\nu^2 T_2^2}\right), \tag{A7}$$

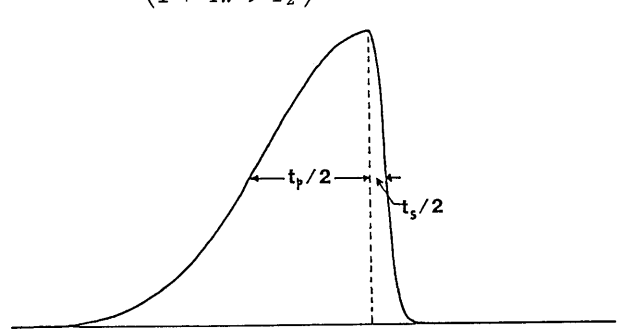

Fig. 11. Truncated pulse characteristic of the plasma shutter output of an OFID laser system. For a transversely excited atmospheric CO_2 laser, t_p is 70 ns and t_s is 10 ps.

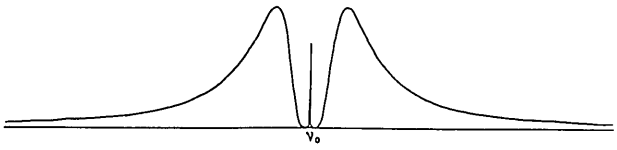

Fig. 12. Numerically computed OFID laser spectrum, corresponding to a temporal pulse duration of 44 ps. For the present calculations the central frequency (ν_0) is equal to 31.25 THz, corresponding to the 9P(26) CO_2 laser transition used for the C_3F_7I experiments of Ref. 9. The peak spectral intensity occurs at 0.8 GHz on either side of the central frequency.

where I_0 is the peak intensity of the temporal pulse profile. The numerically evaluated OFID spectrum (with the peak intensity in the frequency domain normalized to 1) is shown in Fig. 12 for a hot-CO_2 pressure of 100 Torr, implying a temporal pulse duration of 44 ps. The pulse duration is obtained from a careful study of the OFID system.[13] The numerical values used for N, t_p, t_s, and T_2 in this computation are 12.5 Np, 70 ns, 10 ps, and 0.67441 ns (corresponding to a hot-CO_2 temperature of 770 K), respectively. These values are representative of typical operating conditions of this system for data reported earlier.[6,8,9]

From Eq. (A2) we see that the average electric field over the duration of the laser pulse at a frequency ν may be denoted by

$$F_\nu = F(\nu)H(\nu)/\tau_p, \tag{A8}$$

where τ_p is the pulse duration and is equal to 44 ps for the case considered here. The corresponding average intensity (I_ν) may then be calculated readily as

$$I_\nu = |F_\nu|^2 = |F(\nu)H(\nu)|^2/\tau_p^2. \tag{A9}$$

Equations (A9) and (A7) permit a relation between I_ν (the intensity averaged over the pulse duration τ_p at a frequency ν) and I_0 (the peak intensity of the temporal pulse profile).

Explicitly,

$$I_\nu = \frac{\pi I_0}{(8\ln 2)\tau_p^2}\left|\{t_p \exp(-4\pi^2\alpha^2 t_p^2\nu^2)[1 - \phi(2\pi i\alpha\nu t_p)] + t_s \exp(-4\pi^2\alpha^2 t_s^2\nu^2)[1 - \phi(-2\pi i\alpha\nu t_s)]\}\right|^2 \times \exp\left(\frac{N}{1+4\pi^2\nu^2 T_2^2}\right). \tag{A10}$$

REFERENCES

1. T. B. Simpson, J. G. Black, I. Burak, E. Yablonovitch, and N. Bloembergen, "Infrared multiphoton excitation of polyatomic molecules," J. Chem. Phys. **83,** 628–640 (1985).
2. N. Bloembergen and E. Yablonovitch, "Infrared laser-induced unimolecular reactions," Phys. Today **31**(5), 23–31 (1978).
3. P. A. Schulz, Aa. S. Sudbo, D. J. Krajnovich, H. S. Kwok, Y. R. Shen, and Y. T. Lee, "Multiphoton dissociation of polyatomic molecules," Ann. Rev. Phys. Chem. **30,** 379–409 (1979).
4. V. S. Letokhov, *Nonlinear Laser Chemistry—Multiple Photon Excitation* (Springer-Verlag, Berlin, 1983).
5. D. S. King, "Infrared multiphoton excitation and association," in *Dynamics of the Excited State,* K. P. Lawley, ed. (Wiley, New York, 1982), pp. 105–189.
6. P. Mukherjee and H. S. Kwok, "Picosecond laser study of the quasicontinuum of C_2F_5Cl," J. Chem. Phys. **84,** 1285–1295 (1986).
7. A. Yariv, *Quantum Electronics* (Wiley, New York, 1975).
8. P. Mukherjee and H. S. Kwok, "Dynamical temporal evolution of IR absorption spectra observed with picosecond CO_2 laser pulses," J. Chem. Phys. **87,** 128–138, 1987.
9. P. Mukherjee and H. S. Kwok, "On intensity dependent excitation in the room temperature quasicontinuum of C_3F_7I," J. Chem. Phys. **85,** 5041–5044 (1986).
10. E. Yablonovitch and J. Goldhar, "Short CO_2 laser pulse generation by optical free induction decay," Appl. Phys. Lett. **25,** 580–582 (1974).
11. H. S. Kwok and E. Yablonovitch, "30-psec CO_2 laser pulses generated by optical free induction decay," Appl. Phys. Lett. **30,** 158–160 (1977).
12. H. S. Kwok and E. Yablonovitch, "Electrical triggering of an optical breakdown plasma with subnanosecond jitter," Appl. Phys. Lett. **27,** 583–585 (1975); M. Hasselbeck, L. Huang, S. C. Hsu, and H. S. Kwok, "High speed, low-cost laser-triggered plasma shutter," Rev. Sci. Instrum. **54,** 1131–1134 (1983).
13. M. Sheik-bahae and H. S. Kwok, "Characterization of a picosecond CO_2 laser system," Appl. Opt. **24,** 666–670 (1985).